Open Journal of Applied Sciences, 2024, 14, 572-588
https://www.scirp.org/journal/ojapps
ISSN Online: 2165-3925
ISSN Print: 2165-3917

Study of Axisymmetric Infinite Guide Lined with Locally Reacting Material without Flow Using DtN Operators

Boureima Ouedraogo[1], Emmanuel Redon[2]

[1]Department of Physics and Chimistry, C.U. Kaya, Université Joseph Ki-Zerbo, Ouagadougou, Burkina Faso
[2]ESIREM, Université de Bourgogne, Dijon, France
Email: ouedb@yahoo.fr

How to cite this paper: Ouedraogo, B. and Redon, E. (2024) Study of Axisymmetric Infinite Guide Lined with Locally Reacting Material without Flow Using DtN Operators. *Open Journal of Applied Sciences*, **14**, 572-588.
https://doi.org/10.4236/ojapps.2024.142041

Received: January 14, 2024
Accepted: February 26, 2024
Published: February 29, 2024

Abstract

The present work proposed a new method for the modeling by the finite element method of the acoustic propagation problems in infinite axisymmetric cylindrical guides lined with locally reacting absorbent materials without flow. The method deals with the development of an efficient transparent boundary condition based on DtN operators. The method developed in this study is successfully applied to a straight axisymmetric lined guide by imposing a mode on one of the artificial boundaries of the truncated guide. The results are in good agreement with analytical solutions. Applying the method for a non-uniform axisymmetric lined guide which is a complex case, proved its effectiveness and the results compared to those of PML layers are in very good agreement.

Keywords

DtN Operator, Axisymmetric Cylindrical Guides, Finite Element Method, Modes

1. Introduction

Fighting noise pollution is a high order importance for modern societies, especially with the development of the aeronautics, automobile and railway industries. To minimize the noise generated in systems such as aircraft turbojet engines, fans, compressors and automobile exhaust mufflers, several studies have been carried out in recent years to identify noise sources and accurately model the propagation environments of acoustic waves. In most of these systems, before radiating outwards, the noise is channeled by guides of more or less complex geometries (elbows, change of section, presence of obstacles) which can contain fluids whose movement can be more or less rapid depending on the applications (ventilation duct, exhaust lines) and more or less complex (turbulent, laminar, pulsed, etc.). In order to avoid certain phenomena linked to end effects (reflection, radiation at the exit of the guides), the guides are often considered infinite.

In this study, our interest is the acoustic propagation in infinite axisymmetric cylindrical lined guides without flow. The acoustic sources are assumed to be known and we are interested in their radiation in guided environments, neglecting the coupling between acoustic and aerodynamic phenomena which rather concerns the Lighthill analogy [1] [2]. The study of acoustic propagation in guides is an open subject on which several works have been carried out. In most of these works [3] [4] [5], 2D straight guides with or without acoustic treatment on the walls are been considered. Acoustic propagation in these guides is governed by the Helmholtz wave equation. We adopted this equation here because our method of numerical resolution of acoustic propagation problems is based on a modal representation with the acoustic pressure as a scalar unknown. Furthermore, a significant part of our work is devoted to the study of acoustic wave attenuation and absorption. The absorbent material taken into account in this study is of complex local impedance type which is introduced into the wall boundary conditions.

Studying the acoustic propagation in an infinite guide by the finite element method requires truncating the infinite domain by artificial boundaries on which non-reflection conditions must be written. Thus, the most important part of our work concerns the implementation of transparent boundary conditions. A technique often used is the boundary element method (BEM). However, the BEM method requires a Green's function and is better suited for wave propagation problems in infinite space and a homogeneous medium. Another transparent boundary condition called perfectly matched layers (PML) was developed by Béranger [6] for transient problems in electromagnetism. However, PML can be unstable in certain, cases particularly in the presence of inverse modes. On the other hand, PML cannot be produced from physical absorption models and the solution obtained in the layers has no physical reality. In ducted propagation, for a solution using the finite element method, an efficient transparent boundary condition is to consider a boundary condition resulting from a development based on the guide eigenfunctions. The transparent boundary condition of the Dirichlet-to-Neuman (DtN) operator type [7] [8] [9] [10] [11] fitted into this perspective. It's an operator based on a modal decomposition of the acoustic pressure. For a rigid wall duct, the transverse modes are orthogonal in the sense of the usual scalar product; it is then easy to explain the DtN operator. For lined guides, some difficulties occurred. Redon *et al.* [12] in their study for plane problems showed that the eigenvalue problem is no longer self-adjoint for a lined guide even without flow. The DtN operator has been nevertheless established by exploiting the biorthogonality relation existing between the modes [13]. In this study, their works are generalized to explain the DtN operator for axisymmetric problems and we studied the convergence error as a function of the number of modes. Searching modes allowed us in particular to examine the dispersion curves and asymptotic behavior of these modes. It also helped us to establish an orthogonality relation between modes, essential for writing the DtN operator as modal decomposition which the determination of several coefficients (modal and normalization coefficients of transverse modes) is required.

In the following, the problem statement including the equation of acoustic propagation and the appropriate boundary conditions is presented in Section 2. The eigenvalue problem is described in Section 3 including the asymptotic behavior of the modes and their attenuation in the guide. The orthogonality relation between modes is established in Section 4. Then in Section 5, the essential steps leading to implementing the DtN operator for the lined guide are explained and the main numerical results of this study are shown in Section 6.

2. Problem Statement

The space domain is an infinite axisymmetric cylindrical guide with radius R and axis z represented in Figure 1 such that $\Omega_\infty = \{-\infty < z < +\infty, 0 < r < R\}$. Its wall Γ_Z ($r = R$) is covered with an absorbent material characterized by an impedance $Z \in \mathbb{C}$. The equation of the acoustic propagation in the domain is established from the equations of fluid mechanics in the general framework of the thermodynamics of continuous media. We adopted the classic hypotheses of linear acoustics. Viscous constraints and thermal conduction phenomena are assumed to be negligible from an acoustic point of view. All the physical quantities used are functions of Euler variables. The contained fluid in the duct was at rest.

In cylindrical coordinates, the equation of acoustic propagation is given by:

$$\Delta p - \frac{1}{c_0^2}\frac{\mathrm{d}^2 p}{\mathrm{d}t^2} = 0 \tag{1}$$

where p designates the acoustic pressure, c_0 is sound celerity. The operator Δ is the Laplacian in cylindrical coordinates. The boundary condition on the duct axis Γ_0 is a homogeneous Neumann condition [14]:

$$\frac{\partial p}{\partial n} = 0 \tag{2}$$

The boundary condition at the wall Γ_Z is related to the impedance Z by:

$$\frac{\partial p}{\partial n} = ik\frac{p}{Z} \tag{3}$$

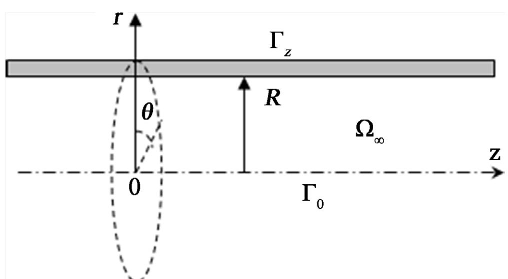

Figure 1. Axisymmetric cylindrical guide with absorbent wall without flow.

For a harmonic regime ($e^{-i\omega t}$) without flow, Equation (1) becomes:

$$\frac{\partial^2 p}{\partial r^2}+\frac{1}{r}\frac{\partial p}{\partial r}+\frac{1}{r^2}\frac{\partial^2 p}{\partial \theta^2}+\frac{\partial^2 p}{\partial z^2}+k^2 p=0 \tag{4}$$

With $k = \omega/c_0$ the wave number. A search for the solution to Equation (4) by the variable separation method while taking into account a convergent solution on the duct axis ($r = 0$) led us to a general solution of the form:

$$p(r,\theta,z)=aA_z J_m(\alpha r)\left(A_\theta e^{im\theta}+B_\theta e^{-im\theta}\right)e^{i\beta z} \tag{5}$$

where a, A_z, A_θ and B_θ are modal coefficients. J_m is a Bessel function of m order, α is a wave number and β is the propagation constant along the z axis. α and β verify the following dispersion equation:

$$\alpha^2 = k^2-\beta^2 \tag{6}$$

Solution of Equation (5) being a harmonic function of the azimuthal variable θ with m the angular mode order and the guide presenting a symmetry of revolution, then the study can therefore be reduced to the plane (r, z). So, the function J_m can be limited to the 0 order, $\varphi(r)=aJ_0(\alpha_{0n}r)$. In order to solve this problem by the finite element method, it is necessary to truncate the infinite domain. We therefore chose two artificial boundaries (Σ− and Σ+) on which transparent boundary conditions should be imposed (see Figure 2).

The boundary conditions on Σ− and Σ+ are both given by:

$$\frac{\partial p}{\partial n}=-T_Z^{\pm}(p) \tag{7}$$

where $T_Z^{\pm}(p)$ represents the DtN operators. To determine these DtN operators the perfect knowledge of the transverse modes of the lined guide and therefore the eigenvalue problem and all essential coefficients are required. This task is carried out in Sections 3 and 4.

3. The Eigenvalue Problem

In this section, we are looking for the acoustic transverse modes of the guide. As shown previously, considering only axisymmetric solutions (*i.e.* $m = 0$, $p(r,z)=\varphi(r)e^{i\beta z}$), the transverse modes $\varphi(r)$ are solutions of:

$$\frac{d^2\varphi}{dr^2}+\frac{1}{r}\frac{d\varphi}{dr}+\left(k^2-\beta^2\right)\varphi=0 \qquad \Omega \tag{8}$$

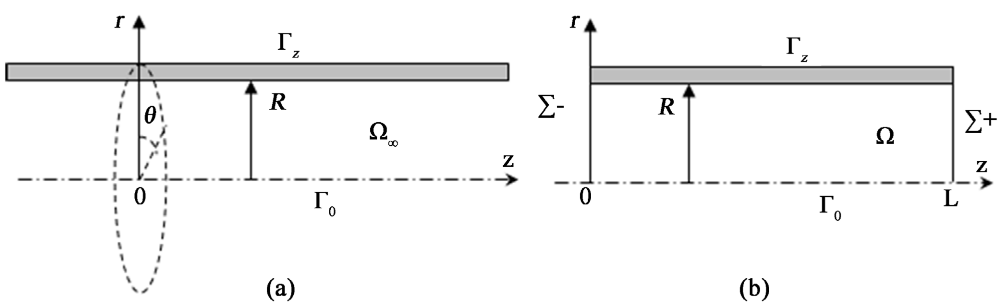

Figure 2. Space domain: (a) Infinite axisymmetric cylindrical guide, (b) truncated guide.

$$\frac{\mathrm{d}\varphi}{\mathrm{d}r} = \frac{ik\varphi}{Z} \qquad \Gamma_Z \tag{9}$$

$$\frac{\mathrm{d}\varphi}{\mathrm{d}r} = 0 \qquad \Gamma_0 \tag{10}$$

where $\varphi(r) = aJ_0(\alpha r)$. The transverse wave numbers α are solutions of the following transcendental equation which depends on the impedance *Z*:

$$-\alpha J_0'(\alpha R) = \frac{ikJ_0(\alpha R)}{Z} \rightarrow -\alpha_n \frac{J_1(\alpha_n R)}{J_0(\alpha_n R)} = \frac{ik}{Z} \tag{11}$$

Note: Although the impedance *Z* of materials is often a function of frequency in physical problems, we considered it constant for simplification. In this study, we determined α_n numerically by the Newton-Raphson algorithm. However, the Newton-Raphson method requires initial values of α_n which are calculated by the finite element method applied in the cross section of the guide. The propagation constants β_n are determined using the following dispersion equation: $\alpha_n^2 + \beta_n^2 = k^2$. **Figure 3** shows the curves of β_n in the complex plane without flow for k = 5 respectively for a rigid guide and a guide with an absorbing wall of impedance *Z* = 1.5 − 1.5i. There are two situations for the rigid guide:

- If $k^2 > \alpha_n^2$, the propagation constant β_n is pure real (see **Figure 3(a)**):

$$\beta_n = \pm\sqrt{k^2 - \alpha_n^2} \tag{12}$$

The mode of order *n* is propagative in the increasing *z* direction: $\beta_n = \beta_n^+$ (respectively in the decreasing *z* direction: $\beta_n = \beta_n^-$). In particular, there is a finite number of propagative modes and the firt mode such as: $\beta_1 = k$ is always propagative.

- If $k^2 < \alpha_n^2$, then the propagation constant is pure imaginary (see **Figure 3(a)**):

$$\beta_n = \pm i\sqrt{\alpha_n^2 - k^2} \tag{13}$$

In this case, the mode of order *n* for $\beta_n = \beta_n^+$ (respectively for $\beta_n = \beta_n^-$) is evanescent in the increasing *z* direction (in the decreasing *z* direction). There are an infinite number of evanescent modes. For $k = \alpha_n$, we define the cut-off frequency of the mode of order *n* (*n* > 1) by: $f_{cn} = \frac{\alpha_n c_0}{2\pi}$.

For the lined guide, the eigenvalues α_n are complex (see **Table 1**), all modes are attenuated. However for each wave number *k* (here *k* = *5*), the imaginary part of β_n became higher than its real part beyond a certain order *n* (here *n* = *2*). The mode is then strongly attenuated. This corresponds to a pseudo-cutting phenomenon (**Figure 3**). The propagative modes and the evanescent modes respectively present a weak imaginary part and a weak real part unlike the rigid guide case where β_n was either pure real or pure imaginary.

Finally, it should be noted that for both hard-wall guide and the lined guide without flow, the eigenvalues α_n are identical in the two directions of propagation (*i.e.* $\alpha_n^+ = \alpha_n^- = \alpha_n$), when the propagation constants β_n are opposite ($\beta_n^+ = -\beta_n^-$)

Table 1. Propagation constants for a rigid guide and a lined guide: $k = 5$; $Z = 1.5 - 1.5i$.

	Rigid guide		Lined guide	
n	α_n	β_n	α_n	β_n
1	0.0000 - 0.0000i	5.0000 + 0.0000i	1.7147 - 0.3899i	4.7150 + 0.1418i
2	3.8317 - 0.0000i	3.2122 + 0.0000i	4.2840 - 0.3397i	2.6574 + 0.5476i
3	7.0155 - 0.0000i	0.0000 + 4.9212i	7.2598 - 0.2205i	0.3039 + 5.2677i
4	10.1734 - 0.0000i	0.0000 + 8.8599i	10.3398 - 0.1582i	0.1807 + 9.0509i
5	13.3236 - 0.0000i	0.0000 + 12.3499i	13.4499 - 0.1226i	0.1320 + 12.4861i
6	16.4706 - 0.0000i	0.0000 + 15.6933i	16.5724 - 0.0998i	0.1047 + 15.8002i
7	19.6158 - 0.0000i	0.0000 + 18.9679i	19.7012 - 0.0841i	0.0870 + 19.0561i
8	22.7600 - 0.0000i	0.0000 + 22.2040i	22.8335 - 0.0727i	0.0745 +22.2794i
9	25.9036 - 0.0000i	0.0000 + 25.4165i	25.9681 - 0.0640i	0.0652 + 25.4822i
10	29.0468 - 0.0000i	0.0000 + 28.6132i	29.1043 - 0.0571i	0.0580 + 28.6716i

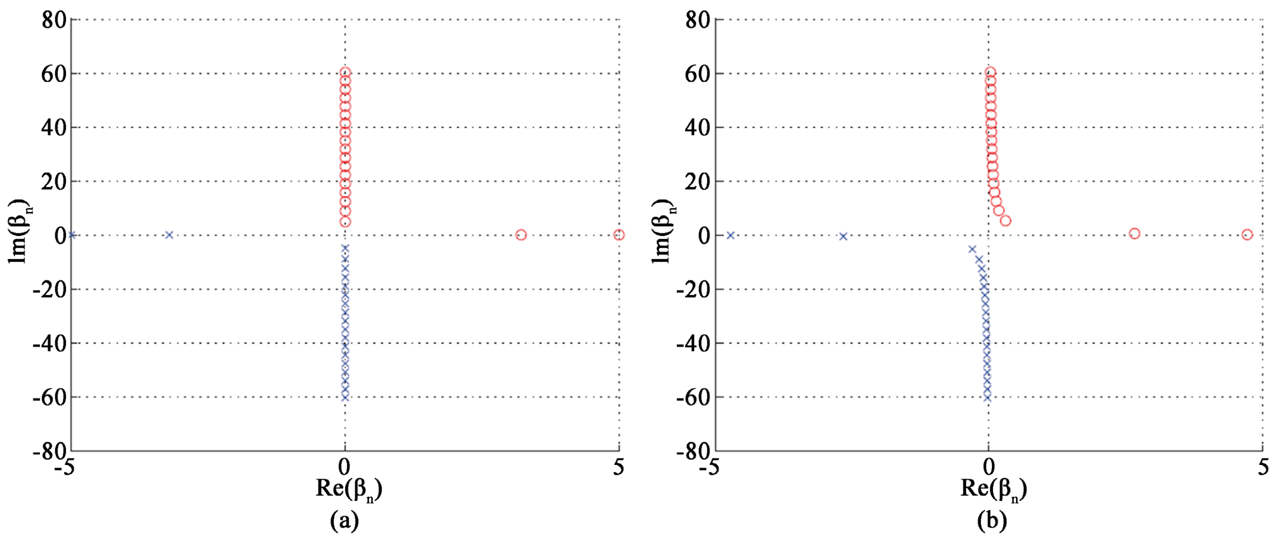

Figure 3. Propagation constants β_n for $k = 5$ in absence of flow: **o** propagative modes following increasing *z*; **x** propagative modes following decreasing *z*. (a) Rigid guide; (b) Lined guide.

as shown in Figure 3.

3.1. Asymptotic Behavior of the Modes

As explained above (see Table 1 and Figure 3), due to the impedance *Z*, the values of α_n and β_n for the lined guide are complex but were tending to those of the rigid guide, especially for the higher order modes. In the Reference [12], it has been proven that for a rectangular 2D lined guide, the modes asymptotically become like those of a rigid guide. The same phenomenon is also observed for an axisymmetric guide. For an axisymmetric rigid guide the boundary condition at the wall is zero meaning $\partial p/\partial n = 0$. This phenomenon can be observed in Figure 4(a), including the higher order modes whose appearance can be seen near the wall in Figure 5(a). For a lined axisymmetric guide, the boundary condition is given in Equation (3) which depends on the impedance *Z*. The normal acoustic velocity and the normal derivative of the pressure are no longer zero at the wall of the guide (see Figure 4(b)).

However, the appearance of the higher order modes near the absorbing wall (Figure 5(b)), showed that the normal derivative of the pressure is becoming zero again meaning that the modes behave asymptotically like those of the rigid guide. This result can be explained using Equation (11). Indeed, as $\lim_{n\to+\infty}|\alpha_n| = +\infty$, so:

$$\lim_{n\to+\infty} \frac{J_1(\alpha_n R)}{J_0(\alpha_n R)} = 0 \tag{14}$$

With $J_1(\alpha_n R) = J_0'(\alpha_n R)$, this means that for high order modes, the α_n correspond to the zeros of the derivative of the Bessel function J_0.

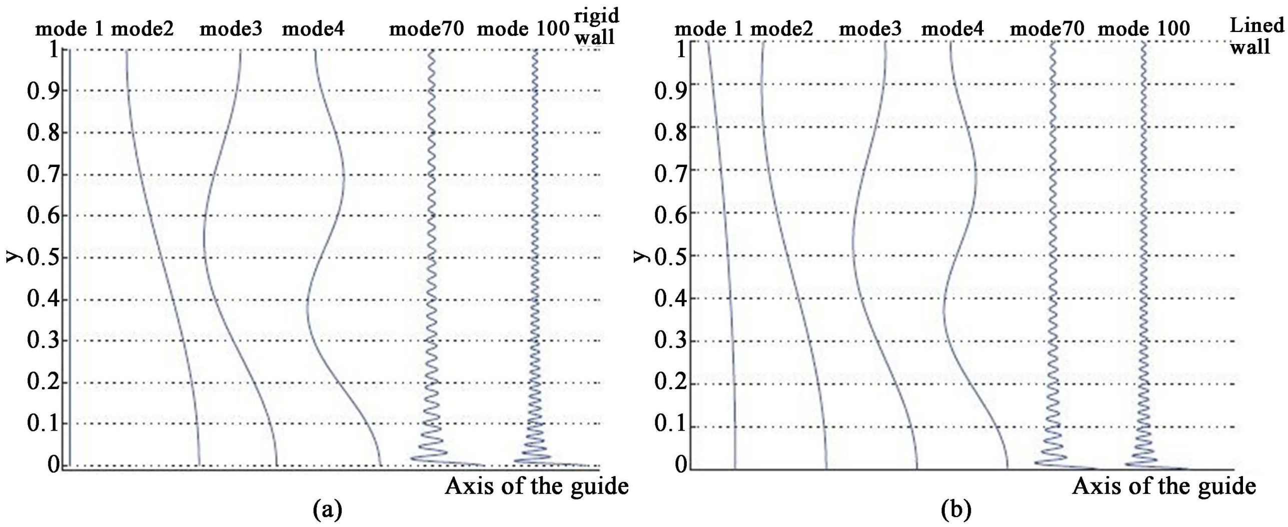

Figure 4. Real part of the pressure in a cylindrical guide for $k = 5$. (a) Rigid guide; (b) Lined guide $Z = 1.5\ (1 - \mathrm{i})$.

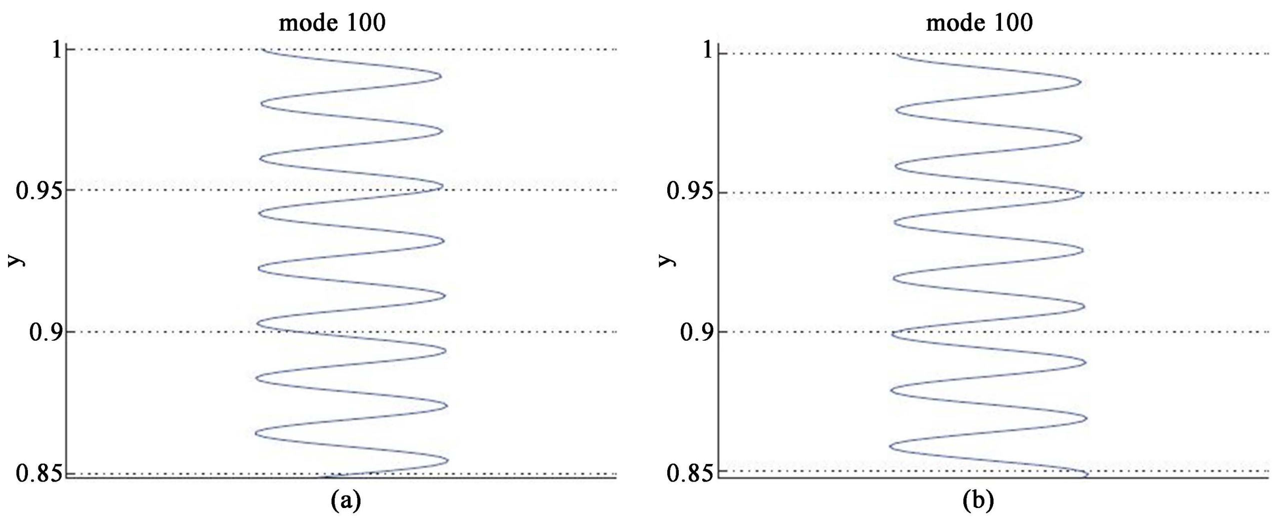

Figure 5. Zoom of the 100th mode for $k = 5$. (a) Rigid guide; (b) Lined guide $Z = 1.5\ (1 - \mathrm{i})$.

The above results are showing that the impact of the absorbent is observed mainly for the first modes of the guide which are propagative but this impact is gradually decreasing for the evanescent modes.

3.2. Phase Speed and Modes Attenuation

In order to fully understand the effect of the impedance Z on the modes, the phase speed and the acoustic attenuation are examined in this section. The phase speed of a wave is its celerity [15]. For a mode of order n, the phase speed is defined along the z axis by:

$$c_{\phi_n} = \frac{\omega}{\beta_n} = \frac{\omega}{\sqrt{k^2 - \alpha_n^2}} \tag{15}$$

For the plane mode (first mode) of a rigid guide $\alpha_1 = 0$, so:

$$c_{\phi_0} = \frac{\omega}{\beta_0} = \frac{\omega}{k} = c_0 \tag{16}$$

The speed of sound c_0 represents the phase speed of the plane wave in a homogeneous medium. For a rigid guide, the phase speed c_{ϕ_n} is always greater than c_0, but tends towards c_0 when ω tends towards infinity (see **Figure 6(a)**). It is infinite for the cut-off frequency f_c (*i.e.* $\omega_c = 2\pi f_c$). This is due to the propagation constant β_n values which are for a rigid guide, purely real for propagative modes and purely imaginary for evanescent modes. However for a lined guide, β_n being always complex (see **Figure 3**), the phase speed curves present a pseudo-cutting phenomenon (see **Figure 6(b)**). The phase speed c_{ϕ_n} no longer tends towards infinity but presents maxima. Furthermore, for a given mode, the imaginary part of β_n is proportional to the attenuation of the mode. Thus, more the material is absorbent; more the propagative modes are attenuated. **Figure 7** presents the imaginary part β_n as a function of ω for a rigid guide and a lined guide with $Z = 1.5(1 - \mathrm{i})$. For both guides, we can see practically

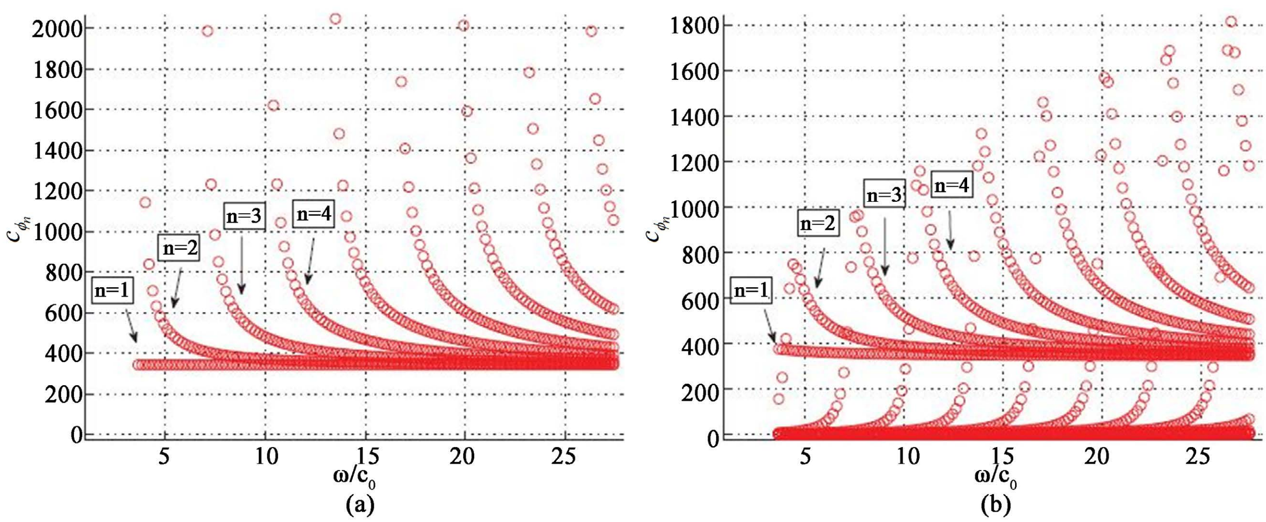

Figure 6. Phase speed c_{ϕ_n} as a function of the pulsation ω in the absence of flow. (a) Rigid guide; (b) Lined guide $Z = 1.5(1 - \mathrm{i})$.

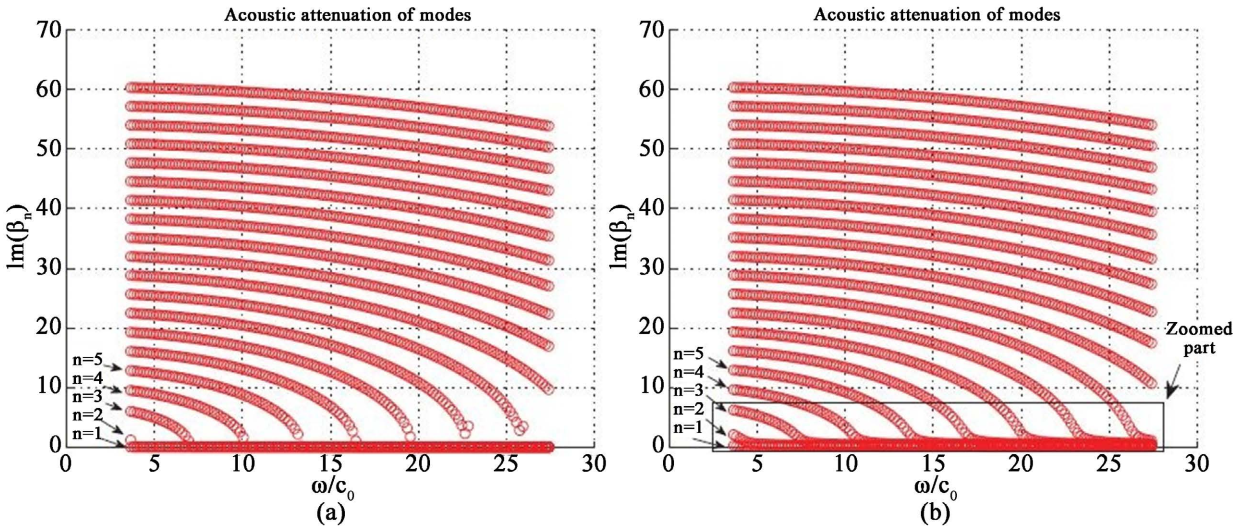

Figure 7. Attenuation of the modes (imaginary part of β_n) as a function of the pulsation ω in the absence of flow. (a) Rigid guide; (b) Lined guide $Z = 1.5\ (1 - \mathrm{i})$.

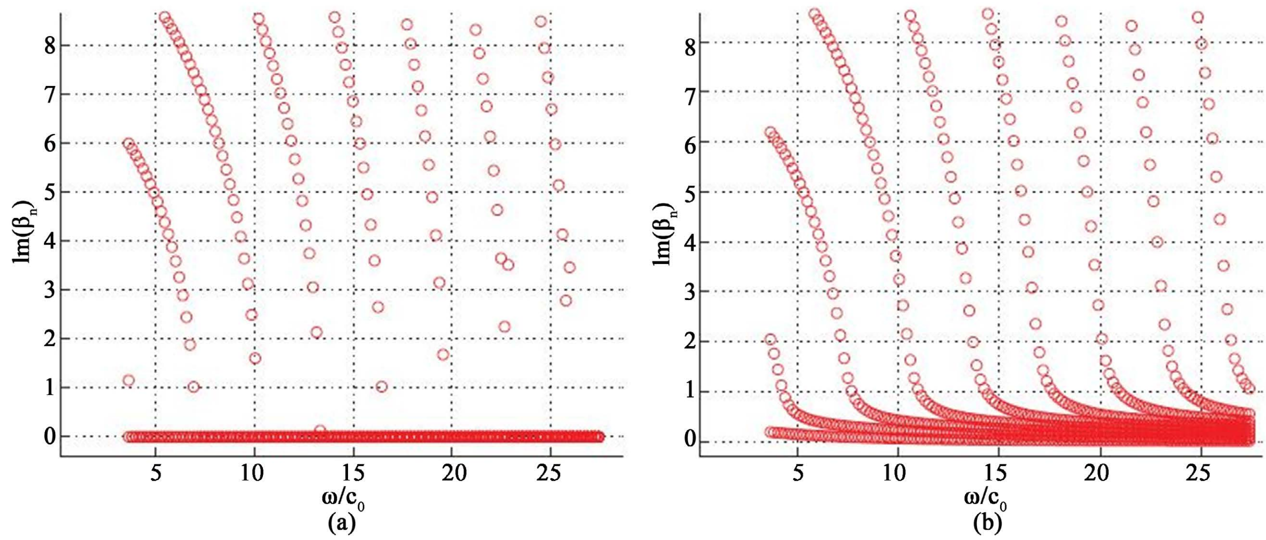

Figure 8. Zoom on the lower part of the curve of the imaginary parts of β_n. (a) Rigid guide; (b) Lined guide $Z = 1.5\ (1 - \mathrm{i})$.

identical curves especially for the high order modes. The difference between the two curves is located on the bottom for the first modes (zoomed part on Figure 8). For the rigid guide, Figure 8(a) shows that the imaginary parts of β_n are zero from the cutoff frequency whereas for the lined guide they are no longer zero as shown in Figure 8(b). This is due to the imaginary part of propagative modes which are not completely zero.

4. Orthogonality Relation and Normalization of the Guide Modes

Knowing the impact of the absorbent on the propagative modes (first modes) and the higher order modes (evanescent modes), an orthogonality relationship between these modes must be defined. Indeed, to write a transparent boundary condition based on a DtN operator, it is necessary to calculate the modal coefficients appearing in the modal decomposition of the acoustic pressure. This is done using an orthogonality relation. This relationship is classic in the case of a rigid guide since the eigenvalue problem is self-adjoint. With absorbent, a different situation arises because the boundary condition on the wall takes into account the impedance *Z*. In their work for a rectangular guide, Redon *et al.* [12] showed that the modes are no longer orthogonal in the sense of the usual scalar product because the eigenvalue problem is no longer self-adjoint [14]. To be able to determine our modal coefficients, we use the biorthogonality relation existing between the modes for non-self-adjoint problems [13]. It is defined by:

$$\left(\varphi_n,\varphi_m\right)_\Sigma^* = \int_\Sigma \varphi_n\varphi_m r\mathrm{d}r = 0 \quad \text{for } m \neq n \tag{17}$$

where $\varphi_n(r)$ is a transverse mode of order *n*, $\varphi_n(r) = a_n J_0(\alpha_n r)$. Its norm is calculated according to the relation in Equation (17). According to Abramowitz and Stegun [16], it is given by:

$$\left(\varphi_n,\varphi_n\right)_\Sigma^* = \int_0^R \varphi_n\varphi_n r\mathrm{d}r = 1 = a_n^2\frac{R^2}{2}\left[J_0^2(\alpha_n R)+J_1^2(\alpha_n R)\right] \tag{18}$$

The normalization coefficients a_n are therefore given by:

$$a_n = \frac{1}{R}\sqrt{\frac{2}{J_0^2(\alpha_n R)+J_1^2(\alpha_n R)}} \tag{19}$$

This normalization is only possible if:

$$J_0^2(\alpha_n R)+J_1^2(\alpha_n R) \neq 0 \tag{20}$$

The discrete values α_n^c roots of Equation (20) are associated with critical values of the impedance Z_n^c which had already been discussed in the 2D case [17]. According to Equation (11), we define a function:

$$S(\alpha_n) = \alpha_n\frac{J_1(\alpha_n R)}{J_0(\alpha_n R)} + \frac{ik}{Z} \tag{21}$$

Having as derivative: $S'(\alpha_n) = \frac{\alpha_n R}{J_0^2(\alpha_n R)}\left[J_0^2(\alpha_n R)+J_1^2(\alpha_n R)\right]$. This implies that $S(\alpha_n^c) = S'(\alpha_n^c) = 0$. The critical eigenvalues α_n^c are therefore double roots of Equations (11) and (20). To determine the critical impedances for a given wave number *k*, we first calculate the roots of Equation (20) and deduce Z_n^c using the transcendental Equation (11). The search for critical impedances is more complicated here than the case of a 2D rectangular guide, because the modes are expressed by Bessel functions. The Bessel functions J_0 and J_1 being continuous on $\mathbb{R}$, we take h_c a complex function and $\alpha_n R = x + iy$. We must therefore resolve:

$$h_c(x,y) = J_0^2(x+iy)+J_1^2(x+iy) = 0 \tag{22}$$

The functions J_0 and J_1 are known even and odd respectively, but their squares are even. This means that the sum of the squares of J_0 and J_1 is also even. So, if the couple (x, y) is a solution of Equation (22), then the couples $(-x, y)$, $(x, -y)$ and $(-x, -y)$ are also solutions of Equation (22). The study can therefore be limited to $x \geq 0$ and $y \geq 0$. To determine the zeros of Equation (22), we chose x and y such that the function h_c is close to 0. These values of x and y are then refined by the Newton-Raphson method to find the exact values for which the function h_c vanishes. The critical impedances Z_n^c are then calculated using the transcendental relation in Equation (11):

$$Z_n^c = -ik \frac{J_0\left(\alpha_n^c R\right)}{\alpha_n^c J_1\left(\alpha_n^c R\right)} \tag{23}$$

Table 2 indicates the real and imaginary parts of α_n^c and the critical impedances calculated for a wave number $k = 5$ and for the following intervals of x and y chosen so that the function h_c is close to 0: $x \in [0, 25]$ and $y \in [0, 5]$. For these intervals of x and y, we obtained seven decreasing critical impedances (see **Figure 9**).

These impedance values make impossible the normalization of the transverse modes φ_n, so Z is chosen in such we can be able to calculate the coefficients α_n and subsequently be able to determine the operators DtN.

5. Determination of the Transparent Boundary Condition

As seen previously in **Figure 2**, to allow discretization by the finite element method, the domain is truncated by artificial boundaries Σ− and Σ+. The boundary conditions on these boundaries are given by the DtN operators already mentioned in Equation (7): $\frac{\partial p}{\partial n} = -T_Z^{\pm}(p)$. The DtN operator being based on a modal decomposition of the acoustic pressure on the boundaries Σ± which truncate the physical domain, the biorthogonality relation in Equation (17) which made it possible to normalize the modes of the guide will also make it possible to determine the modal coefficients resulting of this decomposition. In front of Σ+, we got this:

$$\forall z \geq L, \quad p(r, z) = \sum_{n=0}^{+\infty} A_n^+ \varphi_n(r) \mathrm{e}^{i\beta_n^+(z-L)} \tag{24}$$

Table 2. Critical eigenvalues α_n^c and critical impedances Z_n^c for $k = 5$ and $R = 1$.

n	$Re(\alpha_n^c)$	$Im(\alpha_n^c)$	$Re(Z_n^c)$	$Im(Z_n^c)$
1	2.980382	1.279603	−1.416523	0.608173
2	6.175153	1.618717	−0.757636	0.198602
3	9.341961	1.818873	−0.515672	0.100401
4	12.498507	1.961460	−0.390432	0.061273
5	15.650104	2.072310	−0.313981	0.041576
6	18.798912	2.163011	−0.262498	0.030203
7	21.945980	2.239772	−0.225484	0.023012

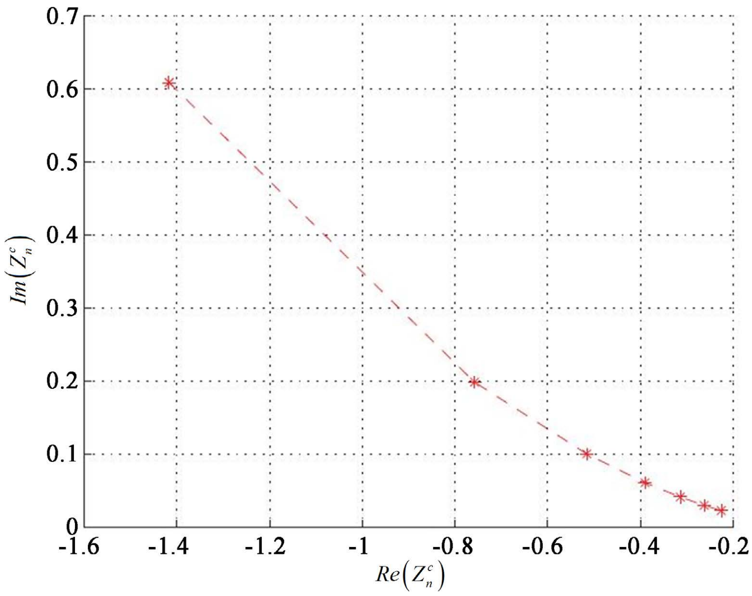

Figure 9. Critical impedances Z_n^c for $k = 5$.

In particular on $z = L$, it became:

$$p(r, z = L) = \sum_{n=0}^{+\infty} A_n^+ \varphi_n(r);\ \ 0 \le r \le R \tag{25}$$

A product of p and a transverse mode $\varphi_n(r)$ using the biorthogonality relation Equation (17), led to the expressions of the modal coefficients A_n^+:

$$A_n^+ = (p, \varphi_n)_\Sigma^* \tag{26}$$

By replacing A_n^+ in Equation (25) and making a derivation about z, we deduced the operator DtN on Σ+:

$$\begin{aligned} &\frac{\partial p}{\partial z}(r, L) = -T_Z^+(p) = \sum_{n=0}^{+\infty} i\beta_n^+ (p, \varphi_n)_\Sigma^* \varphi_n(r) \\ &\to T_Z^+(p) = -\sum_{n=0}^{+\infty} i\beta_n^+ (p, \varphi_n)_\Sigma^* \varphi_n(r) \end{aligned} \tag{27}$$

By similar development, we found on Σ−:

$$T_Z^-(p) = \sum_{n=0}^{+\infty} i\beta_n^+ (p, \varphi_n)_\Sigma^* \varphi_n(r) \tag{28}$$

The determination of the DtN operators completes all the boundary conditions of the equation of the acoustic propagation in the lined guide. We can therefore carry out numerical simulations for some practical examples.

6. Numerical Results

In the following, numerical results obtained by the finite element method of acoustic propagation problems in an axisymmetric cylindrical lined guide, will be presented. The absorbing material is taken to be a complex impedance $Z = 1.5(1 - i)$ and the fluid is at rest.

6.1. Straight Axisymmetric Guide

As a first example we consider the simple case of a semi-infinite straight axisymmetric cylindrical guide lined by an absorbing material with impedance Z = 1.5 (1 − i). By imposing a transverse mode $\varphi_n(r)$ on Σ− and a transparent boundary condition on the Σ+, we compared the numerical solution to the analytical solution: $p_n(r,z)=\varphi_n(r)\mathrm{e}^{i\beta_n z}$.

The truncated guide has the following dimensions: R = 1 and L = 5 (see Figure 10). The propagation equation and boundary conditions are given by:

$$\Delta p+k^2 p=0 \qquad \Omega \tag{29}$$

$$\frac{\partial p}{\partial n}=\frac{ik}{Z}p \qquad \Gamma_Z \tag{30}$$

$$\frac{\partial p}{\partial n}=0 \qquad \Gamma_0 \tag{31}$$

$$p=g \qquad \Sigma- \tag{32}$$

$$\frac{\partial p}{\partial n}=-T_Z^+(p) \qquad \Sigma+ \tag{33}$$

where g is an imposed mode $\varphi_n(r)$. To write the variational formulation associated with the problem in Equation (29), we considered $\psi\in H^1(\Omega)$ a regular test function such that ψ = 0 on Σ−. By multiplying this equation by ψ and integrating over the domain Ω we had:

$$\int_\Omega\left(\Delta p+k^2 p\right)\psi r\mathrm{d}r\mathrm{d}z=0 \tag{34}$$

By applying Green's theorem, the previous integral became:

$$\int_\Omega\left(-\nabla p\cdot\nabla\psi+k^2 p\psi r\right)\mathrm{d}r\mathrm{d}z+\int_{\Gamma_0\cup\Gamma_Z}\frac{\partial p}{\partial n}\psi r\mathrm{d}\Gamma+\int_{\Sigma+}\frac{\partial p}{\partial n}\psi r\mathrm{d}\Sigma=0 \tag{35}$$

where $\partial p/\partial n=\nabla p\cdot n$. By introducing the boundary conditions in Equations (30), (31) and the boundary conditions on the artificial boundary Σ+ in Equation (33), the variational formulation is given by: find $p\in H^1(\Omega)$ such that $\forall\psi\in H^1(\Omega)$ and ψ = 0 on Σ−, we have:

$$\int_\Omega\left(\frac{\partial p}{\partial r}\frac{\partial\psi}{\partial r}+\frac{\partial p}{\partial z}\frac{\partial\psi}{\partial z}-k^2 p\psi\right)r\mathrm{d}r\mathrm{d}z+\frac{ik}{Z}\int_{\Gamma_Z}p\psi r\mathrm{d}\Gamma+\int_{\Sigma+}T_Z^+(p)\psi r\mathrm{d}\Sigma=0 \tag{36}$$

For the requirements of the calculation, the domain Ω is meshed with 4916 elements of type P2 (quadratic Lagrange elements). The numerical simulations are carried out with the MELINA library [18]. Figure 11 and Figure 12 show the pressure distribution in the axisymmetric guide when the first and second.

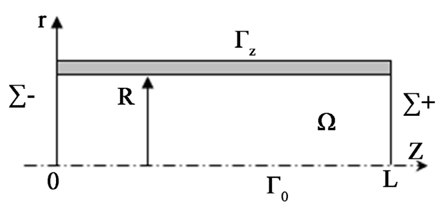

Figure 10. Truncated semi-infinite axisymmetric cylindrical lined guide.

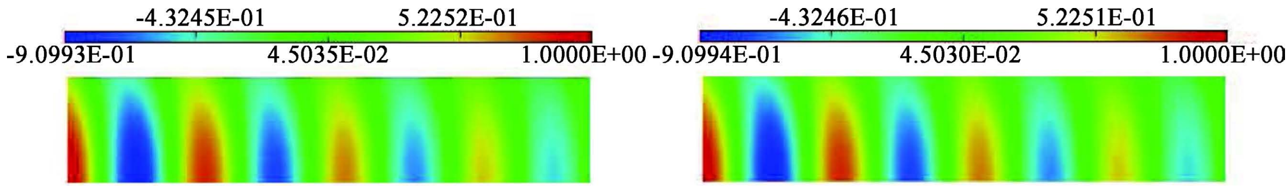

Figure 11. Real part of the pressure for $k = 5$, $Z = 1.5 - 1.5i$, first mode ($\varphi_1(r) = J_0(\alpha_1 r)$) imposed on Σ−: (left) solution with finite elements and DtN, (right) analytical solution.

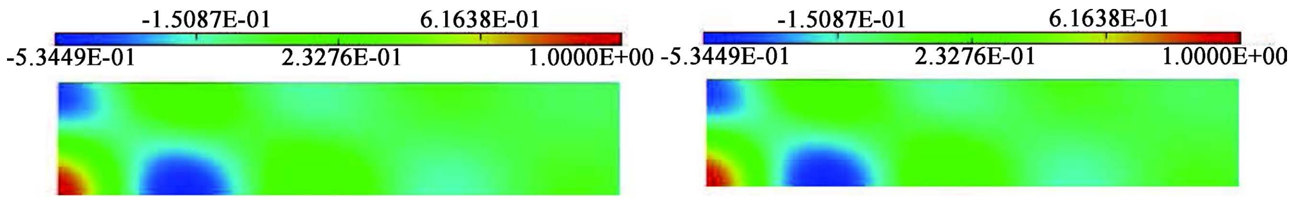

Figure 12. Real part of the pressure for $k = 5$, $Z = 1.5 - 1.5i$, second mode ($\varphi_2(r) = J_0(\alpha_2 r)$) imposed on Σ−: (left) solution with finite elements and DtN, (right) analytical solution.

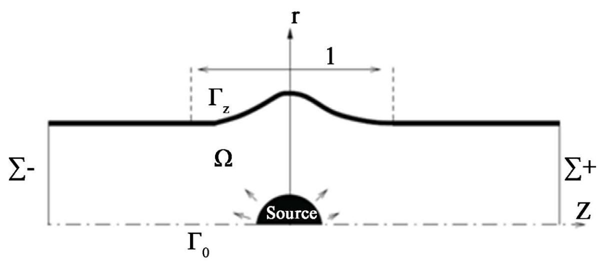

Figure 13. Problem geometry.

transverse modes are imposed respectively on Σ−. The DtN operator on the boundary Σ+ is calculated with 20 modes. We see that the solutions obtained by the finite element method and the DtN operator are very close to the analytical solutions.

For both examples, the relative error in L^2 (Ω) between the numerical and analytical solutions is less than 0.5%. These results proved that the DtN operator is a very good non-reflecting boundary condition of acoustic waves for the truncated infinite guide. For a lined guide, since all the modes are attenuated, if the artificial boundary Σ+ on which the DtN operator is written is located at a sufficiently long distance L from Σ−, it is not necessary to use a transparent boundary condition, the wave being completely attenuated. However, if L is very short, then the modes are not completely attenuated, it is therefore essential to use a transparent boundary condition to avoid reflection of the wave.

6.2. Non-Uniform Axisymmetric Guide

We now present the radiation of a spherical acoustic source located at the center of a portion l of a non-uniform duct lined with an absorbent material of impedance Z This portion l is inserted between two infinite ducts of constant section truncated by the boundaries Σ− and Σ+ (see **Figure 13**). It is an example of problems encountered in industrial systems which geometries are often complex. Our method of DtN operator writing can be again applied on such a guide only if the artificial boundaries are located on its straight and uniform parts. For a source f with compact support, the propagation equation and the boundary conditions are given by:

$$\Delta p + k^2 p = f \qquad \Omega \tag{37}$$

$$\frac{\partial p}{\partial n} = \frac{ik}{Z} p \qquad \Gamma_Z \tag{38}$$

$$\frac{\partial p}{\partial n} = 0 \qquad \Gamma_0 \tag{39}$$

$$\frac{\partial p}{\partial n} = -T_Z^{\pm}(p) \qquad \Sigma\pm \tag{40}$$

The variational formulation of problem with the radiation of the source f is given by: find $p \in H^1(\Omega)$ such that $\forall \psi \in H^1(\Omega)$, we had:

$$\begin{aligned} &\int_\Omega \left(\frac{\partial p}{\partial r}\frac{\partial \psi}{\partial r} + \frac{\partial p}{\partial z}\frac{\partial \psi}{\partial z} - k^2 p\psi \right) r\mathrm{d}r\mathrm{d}z + \frac{ik}{Z}\int_{\Gamma_Z} p\psi r\mathrm{d}\Gamma + \int_{\Sigma+} T_Z^{+}(p)\psi r\mathrm{d}\Sigma \\ &- \int_{\Sigma-} T_Z^{-}(p)\psi r\mathrm{d}\Sigma = -\int_{\Gamma_Z} f\psi r\mathrm{d}r\mathrm{d}z \end{aligned} \tag{41}$$

As analytical solutions are not available, the numerical solutions computed by the finite element method and the DtN operator will be compared to solutions coming from the use of PML layers [6]. For the numerical simulations, the space domain including the PML domains and the physical domain is meshed with 2984 P2 elements (Lagrange triangular elements of order 2). Figure 14 and Figure 15 show the distribution of the acoustic pressure in the non-uniform lined guide for $k = 5$ and $k = 9$ respectively. The finite element method and the DtN operator is carried out with the first 20 modes and results are in good agreement with those of PML layers. The relative error in L^2 (Ω) norm between solutions is respectively equal to 0.001046 and 0.000197. The radiated wave is attenuated near the lined wall Γ_Z and the distribution of pressure is symmetrical in the guide

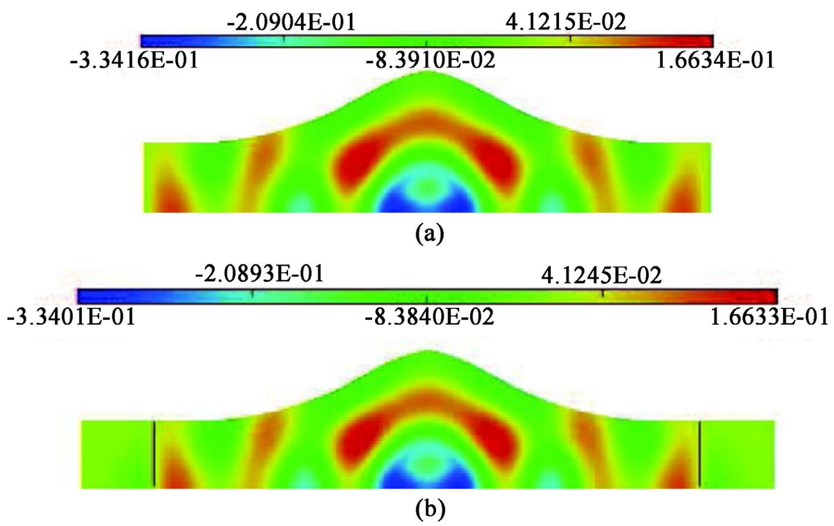

Figure 14. Real part of the pressure for $k = 5$, $Z = 1.5 - 1.5i$: (a) solution with DtN, (b) Solution with PML layers, $\nu = 0.48\ (1 - i)$.

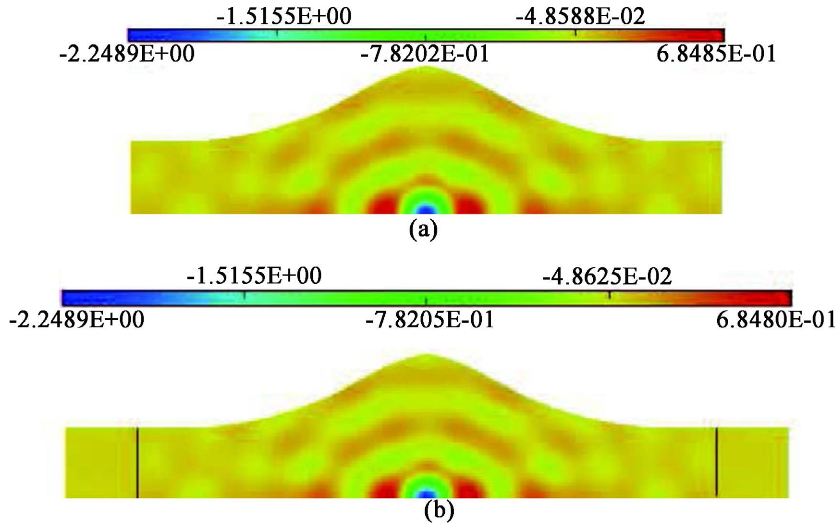

Figure 15. Real part of the pressure for $k = 9$, $Z = 1.5 - 1.5\mathrm{i}$: (a) solution with DtN, (b) Solution with PML layers, $\nu = 0.64\ (1 - \mathrm{i})$.

regarding the source.

7. Conclusion

In this study, we proposed a new method for the modeling by the finite element method of a transparent boundary condition in acoustic propagation problems for infinite axisymmetric cylindrical guides with a wall lined with a locally reacting absorbent material. The transparent boundary condition is carried out with DtN operators which are determined from a decomposition of the acoustic pressure on the guide eigemodes. For a rigid wall, the DtN operator is easy to carry out, but became complex for liner guides. In the case of a lined guide without flow, the modes are no longer orthogonal in the sense of the usual scalar product but there exists a biorthogonality relation which makes it possible to compute the DtN operators. The method developed in this work is successfully applied to a straight axisymmetric lined guide by imposing a mode on one of the artificial boundaries of the truncated guide. The results are in good agreement with the analytical solutions. We then applied the method for a non-uniform axisymmetric lined guide without flow. For this complex case, the method has proven its effectiveness and the results compared to those of PML layers are in very good agreement.

Conflicts of Interest

The authors declare no conflicts of interest regarding the publication of this paper.

References

[1] Lighthill, M.J. (1952) On Sound Generated Aerodynamically. I. General Theory. *Proceedings of the Royal Society of London*, *Series A*, **211**, 564-587. https://doi.org/10.1098/rspa.1952.0060

[2] Lighthill, M.J. (1952) On Sound Generated Aerodynamically. II. Turbulence as a Source of Sound. *Proceedings of the Royal Society of London*, *Series A*, **222**, 1-32. https://doi.org/10.1098/rspa.1954.0049

[3] Harel, P. and Perulli, M. (1971) The Influence of a Stationary Uniform Axial Flow on the Propagation of Acoustic Modes of Vibration in a Cylindrical Duct. *Journal of Sound and Vibration*, **15**, 455-474. https://doi.org/10.1016/0022-460X(71)90405-6

[4] Eversman, W. and Beckemeyer, R.J. (1972) Transmission of Sound in Ducts with Thin Shear Layers—Convergence to the Uniform Flow Case. *The Journal of the Acoustical Society of America*, **52**, 216-220. https://doi.org/10.1121/1.1913082

[5] Rienstra, S.W. and Vilenski, G.G. (2008) Spatial Instability of Boundary Layer along Impedance Wall. 14*th AIAA*/*CEAS Aeroacoustics Conference*, Vancouver, 5-7 May, 1-13. https://doi.org/10.2514/6.2008-2932

[6] Bérenger, J.-P. (1994) A Perfectly Matched Layer for the Absorption of Electromagnetic Waves. *Journal of Computational Physics*, **114**, 185-200. https://doi.org/10.1006/jcph.1994.1159

[7] Keller, J.B. and Givoli, D. (1989) Exact Non-Reflecting Boundary Conditions. Journal of Computational Physics, **82**, 172-192. https://doi.org/10.1016/0021-9991(89)90041-7

[8] Harari, I., Patlashenko, I., and Givoli, D. (1998) Dirichlet-to-Neumann Maps for Unbounded Wave Guides. *Journal of Computational Physics*, **143**, 200-223. https://doi.org/10.1006/jcph.1998.5960

[9] Givoli, D. (2004) High-Order Local Non-Reflecting Boundary Conditions: A Review. *Wave Motion*, **39**, 319-326. https://doi.org/10.1016/j.wavemoti.2003.12.004

[10] Keller, J.B. (204) Artificial Boundary Conditions for Axisymmetric Slow Viscous Flow. *Journal of Computational Physic*, **204**, 399-403. https://doi.org/10.1016/j.jcp.2004.10.027

[11] Grote, M.J. and Keller, J.B. (1995) On Nonreflecting Boundary Conditions. *Journal of Computational Physics*, **122**, 231-243. https://doi.org/10.1006/jcph.1995.1210

[12] Redon, E., Bonnet-Ben, D., Mercier, J.-F. and Poernomo Sari, S. (2011) Non-Reflecting Boundary Conditions for Acoustic Propagation in Ducts with Acoustic Treatment and Mean Flow. *International Journal for Numerical Methods in Engineering*, **86**, 1360-1378. https://doi.org/10.1002/nme.3108

[13] Hazard, C. and Lenoir, M. (1993) Determination of Scattering Frequencies for an Elastic Floating Body. *SIAM Journal on Mathematical Analysis*, **24**, 1458-1514. https://doi.org/10.1137/0524084

[14] Yehya, Y. (1987) Propagation des ondes acoustiques dans les conduites cylindriques de révolution. Ph.D. Thesis, University of Poitiers, Poitiers.

[15] Filippi, P., Habault, D., Lefebvre, J.P. and Bergassoli, A. (1999) Acoustics: Basic Physics, Theory and Methods. *Physics Today*, **52**, 68-69. https://doi.org/10.1063/1.882888

[16] Abramowitz, M. and Stegun, I.A. (1965) Handbook of Mathematical Functions. *Journal of Applied Mechanics*, **32**, 239. https://doi.org/10.1115/1.3625776

[17] Poernomo, S.S. (2008) Propagation acoustique dans les conduits à parois traités en présence d'un écoulement: modélisation par la méthode des éléments finis. Ph.D. Thesis, University of Burgundy, Dijon.

[18] Martin, D. (2007) Librairie mélina. https://anum-maths.univ-rennes1.fr/melina/danielmartin/melina/